Nat Hazards (2015) 77:67–88
DOI 10.1007/s11069-014-1582-9

ORIGINAL PAPER

Mapping climate change-caused health risk for integrated city resilience modeling

Amin M. Owrangi · Robert Lannigan · Slobodan P. Simonovic

Received: 11 November 2014 / Accepted: 26 December 2014 / Published online: 6 January 2015

Abstract Changes in climatic conditions, together with urban population growth, are making the development of tools to help disaster planners and policy makers select mitigation and adaptation measures a priority. The Coastal Cities at Risk (CCaR) project is a multidisciplinary team project involving four large coastal cities: Manila (The Philippines), Bangkok (Thailand), Lagos (Nigeria) and Vancouver (Canada). One of the project objectives includes development of a system dynamics simulation model to assess the resilience of the participating cities to climate change caused by sea level rise and riverine flooding. The resilience model is designed to integrate physical, economic, health, social and organizational impacts of climate change. This paper presents the methodology for providing spatial and temporal information on climate change health impacts for use in the resilience simulator. Basic population data, disease burden and physical conditions are integrated in the development of a composite health impact map. The output of this mapping exercise provides a more fully integrated view of population health to allow for the development of more targeted adaptive and risk reduction strategies at a local level for the City of Metro Vancouver. This methodology has been applied using data for 3 years, 2001, 2006 and 2011 in order to give a dynamic simulation of health impacts using the resilience simulator. The final maps indicate that the Richmond and Delta regions of Metro Vancouver are more vulnerable to climate change caused by sea level rise and flooding compared to other municipalities. The paper demonstrates how composite health impact maps can be used both as an input for resilience modeling, as well as a "stand-alone" product for the assessment and development of mitigation and adaptive strategies for coastal cities.

Keywords Climate change · Coastal cities · Disaster · Resilience · Health · Geographic information system (GIS)

A. M. Owrangi (✉) · S. P. Simonovic
Department of Civil and Environmental Engineering, Western University, London, ON, Canada
e-mail: mowrang@uwo.ca

R. Lannigan
Department of Pathology, Schulich School of Medicine, Western University, London, ON, Canada

1 Introduction

Low-lying coastal, river delta megacities, stressed by fast population growth and economic, social, health and cultural changes, are increasingly vulnerable to climate change. They are exposed to more frequent extreme weather events such as heat waves, heavy rainfall, high winds, sea level rise and storm surges (Simonovic and Peck 2013). Therefore, all coastal cities need to manage these adverse conditions with a combination of climate change mitigation measures and adaptation strategies in order to increase resilience and decrease vulnerability.

According to the fifth assessment report by the United Nation's Intergovernmental Panel on Climate Change from IPCC 2013, one of the major effects of climate change is an increase in the magnitude and frequency of extreme hydrologic events. A number of studies in the Canadian context concur with the findings of the IPCC (2013). A study completed by Environment Canada (2007) on four selected river basins in Ontario using modeling techniques indicates that the impacts of future climate change on the frequency and magnitude of precipitation, stream flow and associated flooding will increase in that part of Canada. The increase in magnitude and frequency of extreme hydrological events, combined with rapid urbanization and land use changes will result in more events like the one experienced by the city of Toronto, Canada, on July 8, 2013. In this event, some parts of the city experienced an extreme downpour (123 mm of precipitation in just 2 h) that left 300,000 people without power, stranded 1,400 people on flooded trains, subway stations, as well as interrupted highway traffic (Nirupama et al. 2014). Many basements were flooded which generated a large amount of damage to personal property and municipal infrastructure. The rainfall affected storm sewer and water drainage systems and created erosion damage to ravines, parks and roadways, all of which resulted in disruption and costs for the city, its residents and businesses in the range of Can $1.2 billion.

Extreme weather events include periods of intensive precipitation of all types (rain, hail or snow), high temperatures, high winds or a combination of these. Over time, populations adapt to the local prevailing climate by behavioral, physiological, cultural and technological responses (McMichael et al. 2006) though extreme events often stress populations beyond current adaptation limits. Physical infrastructure and economic conditions in urban areas are not the only factors that are influenced by climate change. The basic life support systems, such as safe drinking water, clean air, food security and health services are also affected by climate change (Young et al. 2010). The fifth assessment report of IPCC emphasizes that the health impacts of climate change will be a priority challenge for geographically vulnerable populations in the future (IPCC 2013).

Extreme weather events due to climate change have both direct and indirect impacts on health. The direct impacts are mainly personal physical injuries. Indirect effects occur after the event and can take many forms. The direct and indirect impacts on health are subject to population demographics, baseline burden of diseases, geographic location, environmental conditions, socioeconomic factors and the extent of adaptive capacity and mitigation efforts that have been previously achieved. Health impacts depend on the nature of the disaster but include such things as overcrowding in temporary shelters, which can lead to outbreaks of communicable diseases, failure of infrastructure leading to inadequate safe drinking water, food shortages, decreased accessibility to ongoing life support facilities such as cancer care and dialysis etc. In the longer term, mental health problems are being increasingly recognized as a significant problem which can persist long after the initial event (McMichael 2010). These direct and indirect impacts of extreme weather events have a profound effect on the short- and long-term overall health of an urban population which includes physical, mental and spiritual well-being. All these impacts need to be taken into consideration when determining which mitigation and/or adaptation measures would be the most effective in reducing vulnerability (McMichael 2010).

Direct health impacts of extreme weather events generally consist of immediate deaths and physical injuries. Secondary health effects are due to infectious/communicable diseases (types and varieties dependent on geographic location), compromised healthcare access for individuals suffering from non-communicable chronic diseases and mental health conditions (Waroux 2011). The time frames and magnitude of each health impact is also time dependent. Infectious complications, in general, occur early after the event. The effects on non-communicable diseases and mental illness occur somewhat later and can turn into long-term health issues.

Hydrometeorological extremes like floods can have a huge impact on the health of human populations. Since 1900, for example, floods deemed as disasters have led to at least 6.8 million reported deaths and 1.3 million reported injuries across the world (Few and Ahern 2004). Undocumented global health burdens of disease rise annually from floods that are severe in effect but not classified as 'disasters'. Up to the present time, there have been a few published reviews on the health impacts of floods (Hajat et al. 2003; Schmidt et al. 1993), and these have mainly focused on specific geographical regions or are related to specific events.

According to the international disaster database (EM-DAT 2014), out of 6.8 million flood-related deaths (which represents around 20 % of all natural disaster deaths) over 98 % occurred in Asia. The majority of these flood deaths occurred in two catastrophic events in China in 1931 and 1959 (Milly et al. 2002). More recent events which include the tsunami in Japan (2011) and in Indonesia (2004) have also caused significant mortality.

Minimal information is available on the burden of injuries due to flood events. Injuries are not normally reported in most countries, and where injuries are reported, they often cannot be identified specifically as flood related (Milly et al. 2002). The EM-DAT database reports the majority (93 %) of flood injuries occurred in Asia. The injury to death ratio is generally smaller in flooding events than that seen for other disasters (such as wind storms).

The exposure and vulnerability of an urban environment to climate extremes changes with time and in space and depends on many factors. Most of these factors are related to baseline conditions of the overall health of the population, the local economy, social infrastructure, environmental conditions, geography, demographics, cultural values, institutional organization and governance. The United Nations Development Programme (UNDP) and World Health Organization (WHO) are involved with a series of projects to increase the resilience of sectors involved with the health of populations through the development, preparation and the use of warning systems (WHO 2010). For example, one project includes the use of a meteorological-based decision support system for heat waves in China (Chalabi and Kovats 2014).

One of the key objectives of the CCaR (CCaR 2011) project is the development of composite human health impact maps. They can assist in the reduction of uncertainty and streamline the decision making process related to the development and implementation of healthy urbanization policies that will address major human health challenges triggered by the changing climate. The baseline estimation can be provided for each city using generally available estimates, and then these can be modified and refined using specific local knowledge and data. The final product can then be used as (1) input for the resilience model and (2) for the development of stand-alone health impact maps. Both of these can provide direction to planners and policy makers in terms of what mitigation and adaptation strategies would provide the greatest benefit for the community.

The city resilience simulation modeling (Simonovic and Peck 2013) has been adopted in the CCaR project as a tool for the investigation of climate change adaptation options and as a mechanism for the integration of various impacts of climate change-related disasters. There are many definitions of resilience, and the common elements of these definitions include: (1) minimization of losses, damages and community disruption; (2) maximization of the ability and capacity to adapt and adjust when there are shocks to systems; (3) returning systems to a functioning state as quickly as possible; (4) recognition that resilient systems are dynamic in time and space; and (5) acknowledgements that post-shock functioning levels may not be the same as pre-shock levels.

For the purposes of the CCaR project, a flood resilient community is a sustainable network of physical (constructed and natural) systems and human communities (social and institutional) that possess the capacity to survive, cope, recover, learn and transform from flood events by: (1) reducing failure probabilities; (2) reducing failure consequences (for example, material damage); (3) reducing time to recovery; and (4) creating opportunity for development and innovation from adverse impacts. Numerous institutions, organizations and elements in the urban environment contribute to community flood resilience, for example, water and power lifelines, acute care hospitals and organizations that have the responsibility for emergency management. Improving the resilience of critical lifelines is critical for overall community resilience. For example, since no community can cope adequately with a flood disaster without being able to provide emergency care for injured victims, hospital functionality is crucial for community resilience.

The resilience quantification framework has two qualities: inherent (functions well during non-flooding periods) and adaptive (flexibility in response during flood events) and can be applied to physical environment (built and natural), social systems, governance network (institutions and organizations) and economic systems (metabolic flows). An original space–time dynamic resilience measure (STDRM) of Simonovic and Peck (2013) is designed to capture the relationships between the main components of resilience.

STDRM is based on two basic concepts: level of system performance and adaptive capacity. They together define resilience. The level of system performance integrates various impacts (i) of flood on a community. The following impacts [units of resilience (ρ^i)] can be considered: physical, health, economic, social and organizational, but the general measure is not limited to them. Measure of system performance $P^i(t,s)$ for each impact (i) is expressed in the impact units [physical impact may include for example length (km) of road being inundated; health impact may be measured using an integral index-like disability-adjusted life year (DALY); and so on]. This approach is based on the notion that an impact, $P^i(t,s)$, which varies with time and location in space, defines a particular resilience component of a community, see Fig. 1 adapted from (Simonovic and Peck 2013). The area between the initial performance line $P_0^i(t,s)$ and performance line $P^i(t,s)$ represents the loss of system resilience, and the area under the performance line $P^i(t,s)$ represents the system resilience $(\rho^i(t,s))$. In Fig. 1, t_0 denotes the beginning of the flood event, t_1 the end and t_r the end of the flood recovery period.

In mathematical form, the loss of resilience for impact (i) represents the area under the performance graph between the beginning of the system disruption event at time (t_0) and the end of the disruption recovery process at time (t_r). Changes in system performance can be represented mathematically as:

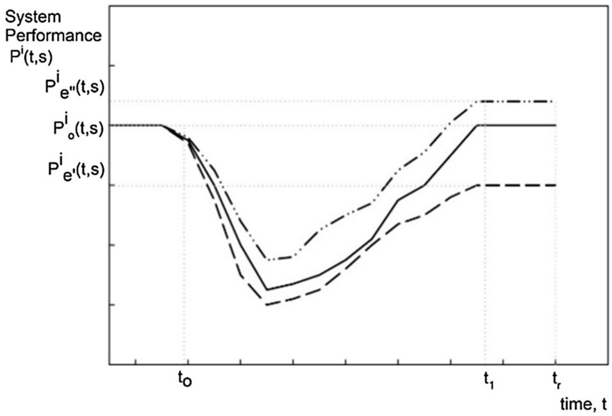

Fig. 1 System performance

$$\rho^i(t,s) = \int_{t_0}^{t} \left[P_0^i - P^i(\tau,s)\right] \mathrm{d}\tau \tag{1}$$

where $t \in [t_0, t_r]$.

When performance does not deteriorate due to disruption, $P_{\mathrm{o}}^i(t,s) = P^i(t,s)$, the loss of resilience is 0 (i.e., the system is in the same state as at the beginning of disruption). When all of system performance is lost, $P^i(t,s) = 0$, the loss of resilience is at the maximum value. The system resilience, $r^i(t,s)$, is calculated as follows:

$$r^i(t,s) = 1 - \left(\frac{\rho^i(t,s)}{P_o^i \times (t - t_o)}\right) \tag{2}$$

As illustrated in Fig. 1, performance of a system which is subject to a flood (disaster event) drops below the initial value, and time is required to recover the loss of system performance. Disturbance to a system causes a drop in system resilience from value of 1 at t_{o} to some value $r^i(t_1, s)$ at time t_1, see Fig. 2. Recovery usually requires longer time than

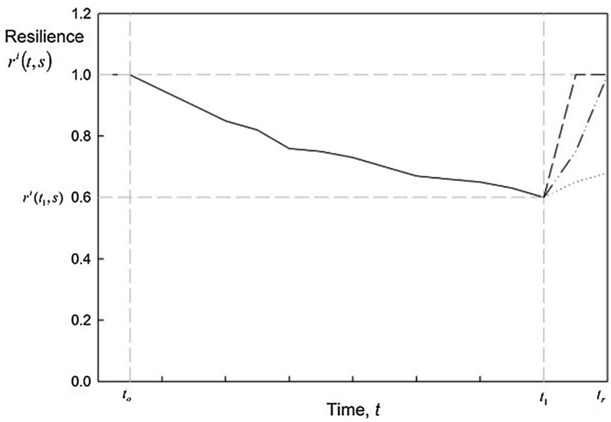

Fig. 2 System resilience

the duration of disturbance. Ideally resilience value should return to a value of 1 at the end of the recovery period, t_r (dashed line in Fig. 2); and the faster the recovery, the better. The integral STDRM [over all impacts (i)] is calculated using:

$$R(t,s) = \left\{ \prod_{i=1}^{M} r^i(t,s) \right\}^{\frac{1}{M}} \tag{3}$$

where, M is the total number of impacts.

In this research, risk is defined as the exposure of the various segments of the population to three different health impacts (communicable and non-communicable diseases, and injuries) of inundation caused by climate change-caused riverine flooding and sea level rise. The main objective of the work presented in this paper includes development of an approach for addressing health impacts of climate change-caused disasters. Health impacts, as presented above are one dimension (i) of the complex city resilience. The presented approach is illustrated by the development of health impact maps of climate change-related flooding for the City of Metro Vancouver. The methodology and its application: (1) provide for major shift in natural disaster management from risk to resilience, from static risk to dynamic spatial resilience, from single impact risk to integrated resilience measure; (2) illustrate how the available data and tools can provide for an effective implementation of the proposed approach; and (3) offer for the first time an integrated health impact assessment for the Metro Vancouver. Data collected by national census in 2001, 2006 and 2011 on social, health and physical conditions have been integrated in the development of the composite health impact maps for these 3 years. The outcome of the mapping exercise provides a new integrated knowledge that can be of assistance in future development of climate change adaptation and disaster risk reduction strategies related to population health for the City of Metro Vancouver.

The rest of the paper is organized as follows. Methods and drivers that have been used in this study are presented in the methodology section. The City of Metro Vancouver case study is then introduced. The discussion of the results is presented after the case study. Finally, a summary of the study is provided, and further research works are outlined.

2 Methodology

Coastal megacities are very complex environments that are vulnerable to several of the negative impacts of climate change. In these environments, a large number of factors impact human health. The methodology presented here uses an interdisciplinary approach to identify, assess and communicate climate change-related health impacts in coastal megacities. The main objective of this methodology was to develop an integrated measure of human health, namely the human health impact, and map its value in time and space. The output of this mapping exercise provides an integrated view of population health for developing more targeted, adaptive and risk reduction strategies at a local level for the City of Metro Vancouver. This methodology has been applied using 3 years of data in order to help the dynamic simulation of health impacts using a resilience simulator. The paper demonstrates how composite health impact maps are used as an input for resilience modeling, as well as "stand-alone" product.

The illustrative presentation of the methodology for the development of health impact map is in Fig. 3. In the first step, the non-physical health impact map, which is the integration of social conditions and the measure of burden of diseases, is created. The

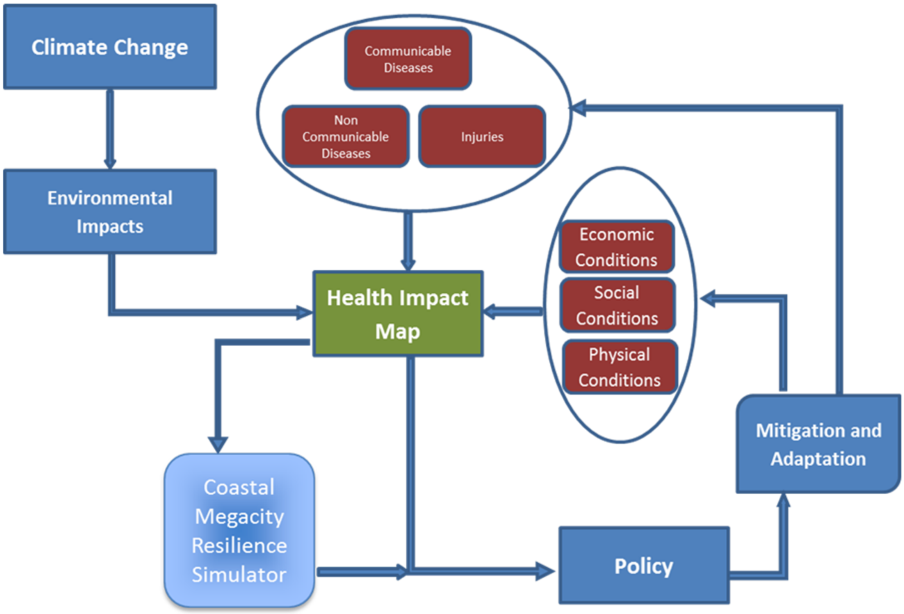

Fig. 3 The illustration of methodology for generating human health impact map

second step is the integration of the non-physical map with the physical (topography) conditions.

The factors included in spatial and temporal mapping process of the health impact are: the physical environment (land elevation); age distribution (total population, population above 65 years of age and population under 4 years of age); and burden of disease by major category (communicable, non-communicable and injuries) expressed as the disability-adjusted life year (DALY) per 100,000 people. DALY combines the number of years of healthy life lost due to premature mortality and disability (WHO 2008). Integrated measure of population health, such as DALY, provides one possible health impact quantification framework. The DALY measures health gaps as opposed to health expectancies. It measures the difference between a current situation and an ideal situation where everyone lives up to the average life expectancy, and in ideal health. Based on life tables, the standard life expectancy at birth is set at 80 years for men and 82.5 for women. The DALY combines the time lived with disability and the time lost due to premature mortality (Prüss-Üstün et al. 2003). It is recognized that the DALY is a relatively crude estimate and is given in the WHO tables as country wide values. More accurate disease statistics are available from Vancouver itself, but this project does include other cities in countries where the availability of data is more limited. The objective was to develop a methodology that could be used by all sites. The DALY tables provide such a baseline and this can be modified or supplemented with local data if required.

2.1 Input data

The human health impact is considered to be a function of physical, disease burden and social vulnerability data.

$$\text{Human Health impact (HHI)} = f(\text{physical conditions, disease conditions, social conditions}) \quad (4)$$

All available data for each city are used as input into a computerized procedure for the computation of a composite human health impact map for each year. All spatial data are collected and presented using a dissemination area, as the spatial unit of analysis (Simonovic 2011). This area is defined by Statistics Canada as a small, relatively stable geographic unit composed of one or more adjacent dissemination blocks. It is the smallest standard geographic area for which all census data are disseminated. Total number of dissemination areas for the City of Metro Vancouver is 3,790, and they differ in size and population density which varies between 0 and 4,515 people per dissemination area.

2.2 Human health impact calculation

The process adopted for this study can be subdivided into four major steps of data collection, data transformation and normalization, data integration and human health impact mapping.

2.2.1 Data collection

The social conditions are assessed using three variables: total population, population of people over age 65 and children under age 4 were taken from Stats Canada, and it is based on census data (Statistics Canada 2012). Children, senior and DALYs are all based on census population data.

The burden of disease integrates communicable diseases, non-communicable diseases and injuries. WHO defines communicable diseases as: “Infectious diseases caused by pathogenic microorganisms, such as bacteria, viruses, parasites or fungi; the diseases can be spread, directly or indirectly, from one person to another” (WHO 2008). Also, non-communicable disease is a medical disorder or disease, which by definition is non-infectious and non-transmissible between people (Lim et al. 2010). The WHO reports non-communicable diseases to be undoubtedly the primary cause of death in the world, representing over 60 % of all deaths. Topography of the Vancouver region was obtained from the Canadian Digital Elevation Data database (CDED 2013). The individual spatial data from social conditions, burden of disease and physical conditions are integrated using the GIS to generate the final human health impact map.

2.2.2 Data transformation and normalization

Raw data are first rescaled by using linear scale transformation methods and then normalized. A number of linear scale transformations exist in the literature (Massam 1988). The two procedures used here are presented in Eqs. 5 and 6. For normalizing the data, each data raw data are divided by the maximum value for a given category according to:

$$x'_{ij} = \frac{x_{ij}}{x_j^{\max}} \quad (5)$$

or

$$x'_{ij} = 1 - \frac{x_{ij}}{x_j^{\max}} \quad (6)$$

where x'_{ij} is the normalized score for the ith category and the jth variable, x_{ij} is the variable value, and $x_j^{\max}$ is the maximum value for the jth variable. The value of normalized data ranges from 0 to 1. The higher the value, the higher the risk. Equation 5 is used when the extent of risk is directly correlated with the variable value (i.e., total population, senior population, children population, communicable and non-communicable diseases and injuries). Equations 7, 8 and 9 are used in calculation of the normalized population (PopN), normalized senior population (SenN) and normalized children population (ChildN), respectively.

Since the risk of climate change-caused hazards is higher for higher population density, Eq. 7 was used to normalize the population. A number closer to 4,515 (maximum population in one Metro Vancouver dissemination area) is associated with a higher risk, since it is closer to one. The same approach is used for other variables.

$$\text{PopN} = \frac{\text{Pop.}}{\text{Max Pop.}} \quad (7)$$

$$\text{SenN} = \frac{\text{Senior Pop.}}{\text{Max Senior Pop.}} \quad (8)$$

$$\text{ChildN} = \frac{\text{Child Pop.}}{\text{Max Child Pop.}} \quad (9)$$

where Pop is population for each dissemination area, Max Pop is the maximum population per dissemination area for the entire city, and the units of both are number of people. Senior Pop is the population of senior people above 65 years old per dissemination area, Max Senior Pop is the maximum senior population per dissemination area for the whole city, and both their units are number of people. Finally, Child Pop is the number of children (under 4 years old) per dissemination area, Max Child Pop is the maximum children population per dissemination area for the entire metropolitan area, and the units of them are number of people.

Equations 10, 11 and 12 are used for calculation of normalized communicable (CatIN) and normalized non-communicable diseases (CatIIN), and normalized injuries (CatIIIN) based on the WHO national based DALY tables.

$$\text{CatIN} = \frac{\frac{\text{Pop}}{100{,}000} \times \beta}{\text{Max}\left(\frac{\text{Pop}}{100{,}000} \times \beta\right)} \quad (10)$$

$$\text{CatIIN} = \frac{\frac{\text{Pop}}{100{,}000} \times \gamma}{\text{Max}\left(\frac{\text{Pop}}{100{,}000} \times \gamma\right)} \quad (11)$$

$$\text{CatIIIN} = \frac{\frac{\text{Pop}}{100{,}000} \times \lambda}{\text{Max}\left(\frac{\text{Pop}}{100{,}000} \times \lambda\right)} \quad (12)$$

where Pop is the total number of people in each dissemination area, and β is communicable DALY rate for the country, and it is 601 based on the WHO table. γ is non-communicable

DALY rate, and λ is injury DALY rate. For Canada, γ is 8,799 and λ is 920 (WHO 2008). For the City of Metro Vancouver, Canada's data were used.

If the measure is of the minimization type (i.e., the lower the value, the higher the risk, like for example ground elevation), Eq. 6 is used in the normalization process. The normalized value of the ground elevation (TopoN) is calculated according to Eq. 13.

$$\text{TopoN} = 1 - \frac{\text{Elevation}}{\text{Max Elevation}} \tag{13}$$

2.2.3 Data integration

The integration is performed on two levels. First, non-physical impacts integrated into one map, and then it has been integrated with physical condition. The following general equation (Eq. 14) is used to integrate all the available data:

$$\text{HI} = \alpha_1\left(\sum_1^n W_i \times \text{NP}_i\right) + \alpha_2\left(\sum_1^m W_i \times P_i\right) \tag{14}$$

where NP is the representation for non-physical data, Wi is the weight of each variable considered, P_i is the available physical data, and α_1 and α_2 are weights associated with non-physical and physical data inputs, respectively. Introduction of a double weighting scheme allows for active participation of decision makers in the development of a human health impact map. Selection of different weights can be used to (a) represent different preferences of decision makers and (b) assess the impact of each input on the final value of the human health impact.

Based on the general equation and available data, Eq. 15 was used for the City of Metro Vancouver. $W1$–$W6$ are weighted equal, and the value is 1/6 and $W7 = 1$ in this study. Value of 0.5 has been selected for α_1 and α_2 in this case study because there is no other study in the literature which can help the weighting system at this level. The results will give a basic but comprehensive idea about equal weights scenario.

$$\text{HI} = 0.5\left[\frac{w1 \times \text{PopN} + \text{w2} \times \text{SenN} + \text{w3} \times \text{Child} + \text{w4} \times \text{CatIN} + \text{w5CatIIN} + \text{w6CatIIIN}}{\sum_{k=1}^{6} w} + w7 \times \text{Topo}\right] \tag{15}$$

2.2.4 Human health impact mapping

After transforming and normalizing all of our available inputs, the weighting procedure can be easily implemented in the GIS environment before the integration. The resulting map provides an integrated view of population health for this region, information which may help in developing more targeted adaptation and risk reduction strategies at a local level. Empirical applications suggest that the weighting method is one of the most effective techniques for spatial decision making including GIS based approaches (Malczewski et al. 1997).

2.3 Case study

The Organization for Economic Co-operation and Development (OECD) estimated the average global flood damages in 2005, at about US$6 billion per year, could rise to US$52 billion by 2050 with expected socioeconomic change alone (OECD 2013). The cities classified at high risk today, as measured by annual average losses because of floods in developed and developing countries include: Guangzhou and Shenzhen in China; Miami, New York, New Orleans and Boston in the United States; Mumbai in India; Nagoya and Osaka-Kobe in Japan; and Vancouver is the only Canadian city (OECD 2013).

The City of Metro Vancouver includes 24 local municipalities and authorities situated in the southwest corner of British Columbia, Canada (Fig. 4). Port Metro Vancouver is Canada's largest port by tonnage of commodities handled (OECD 2013). Municipalities located along the coastline or on the Fraser River Delta are vulnerable to sea level rise and fresh water flooding. Sea level flooding has affected many parts of Metro Vancouver, including: the District of West Vancouver, the District and City of North Vancouver, the City of Vancouver, the City of Richmond, the Corporation of Delta and the City of Surrey. Given its low elevation and exposure to the sea, the Corporation of Delta experienced the most significant flooding and flood damage in the past (Forseth 2012).

Vancouver's history includes a number of disaster events (Fig. 5) that were caused by sea level rise storm surge and flash flooding. The two most significant events of this type are the October 12th, 1962 landfall of Typhoon Freda and the February 4th, 2006 storm surge event that affected the Corporation of Delta. Figure 5 provides a timeline of historical extreme weather events in the City of Metro Vancouver (Forseth 2012).

The country based statistics data are used for the city in order to standardize the methodology for the application with all CCaR project cities. In most cases (Canada included), the majority of the population lives in urban areas. Therefore, the country DALY estimates are pretty close to the urban estimates. If local data are available, it would be possible to modify the numbers used for the country. For example, if it is known that there is an area of the city in which the HIV numbers are known to be three times the national average it is possible to include that.

Vancouver (in fact British Columbia in general) has the population data BC database (Popdata 2014) that can provide more accurate data. However, the prohibitively high cost

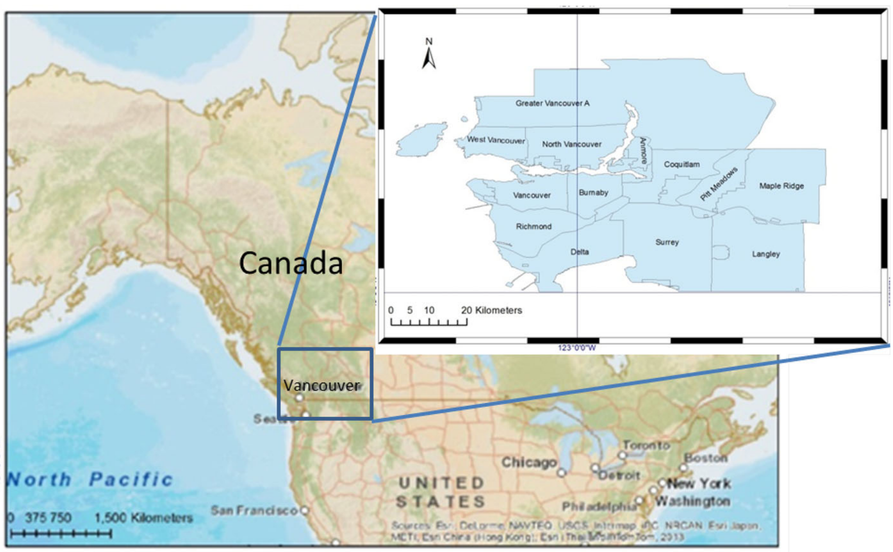

Fig. 4 The City of Metro Vancouver, British Columbia, Canada (ESRI 2014)

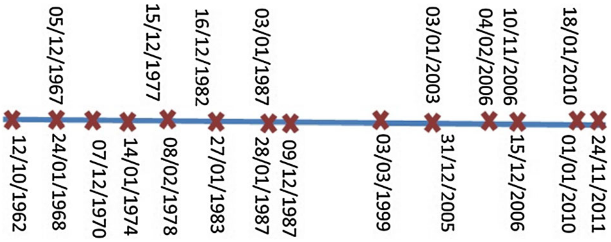

Fig. 5 Timeline of sea level rise storm surge and flash flooding events that affected the City of Metro Vancouver between 1962 and 2012 (Forseth 2012)

prevented its use in this study. Using the crude DALY estimates is sufficient for the assessment of a baseline health measure and provides a similar input into the resilience model for each city.

3 Results

3.1 Population

The city of Metro Vancouver has experienced major transformation in population size, development patterns, economic conditions and social characteristics. Social, economic and built-environment changes have altered the population vulnerability in many ways. Over the last several decades, Metro Vancouver has achieved a significant level of socioeconomic development. In that period, Metro Vancouver's economic expansion has outperformed the Canadian economy. As a consequence (Statistics Canada 2012), employment in Greater Vancouver reached 1.1 million in 2006, and that represents the fastest pace of job growth among Canada's three largest metropolitan areas (Toronto, Vancouver and Montreal) (Turcotte and Schellenberg 2006).

Rapid socioeconomic development has been followed by two parallel trends of considerable population growth and rapid urbanization. In 2011, Metro Vancouver had a population of 2,476,328, while the regional district has a land area of 2,882.55 km^2 and population density of 856.2 people/km^2 (Statistics Canada 2012). In contrast, Metro Vancouver's population in the year 1981 was 1,169,831 (Fig. 6). This shows an increase of more than 100 % over four decades (Statistics Canada 2012).

Fig. 6 Population growth for the City of Metro Vancouver

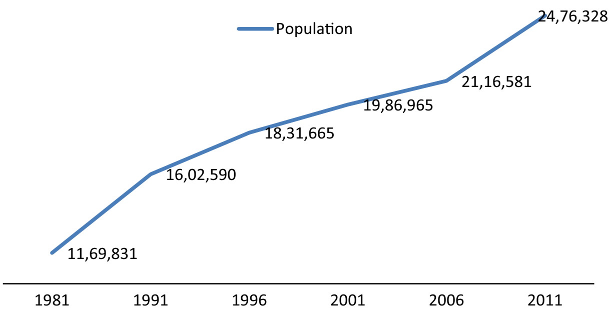

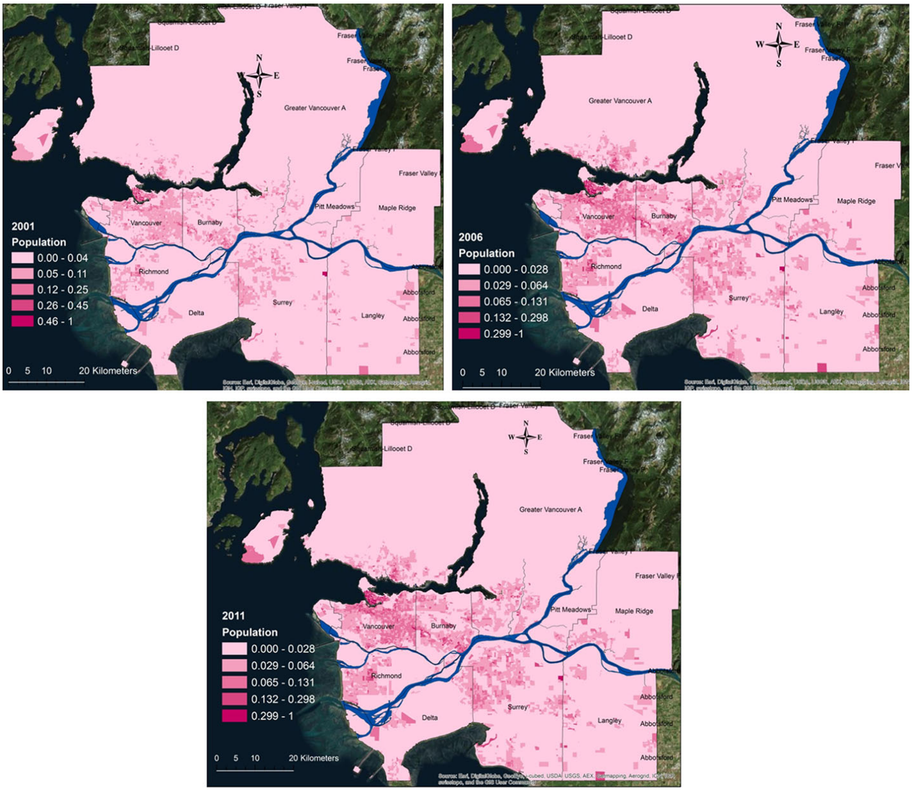

Fig. 7 Calculated normalized population density for the City of Metro Vancouver for 2001, 2006 and 2011

To improve response to potential climate change-caused disasters, it is essential to identify the variability in the vulnerable populations exposed to hazards and to develop consequent adaptation strategies. Figure 7 shows the PopN distribution over the City of Metro Vancouver for 2001, 2006 and 2011. Maps are based on dissemination areas. The map in Fig. 7 shows the PopN density (value between 0 and 1). Numbers closer to one represent a higher density of population. The dark gray regions showing the areas with higher density are mostly located in the City of Vancouver, Richmond and Delta. Based on different scholarly reports, it is clear that high-density population neighborhoods in municipalities may have difficulties in terms of obtaining necessary health services for people after disaster events. For example, the destruction of the transportation infrastructure may prevent provision of health services for many people (Dilley 2005). Therefore, future development decisions should be made taking into consideration the uneven spatial population densities as these may have a significant impact on the level of health risk.

3.2 Senior population

Figure 8 represents the 65 years and older PopN density distribution of the City of Metro Vancouver for the same years. It is also based on dissemination areas. As an example, the

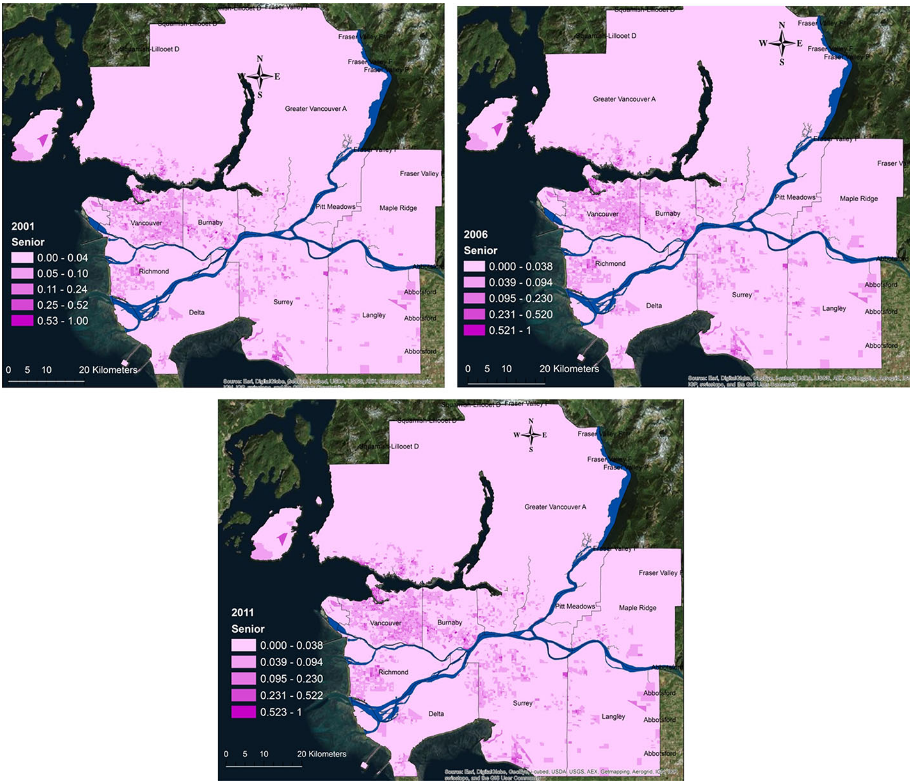

Fig. 8 Calculated normalized senior population density for the City of Metro Vancouver for 2001, 2006 and 2011

population varies between 0 and 790 people per dissemination area for 2011. The density value is normalized (between 0 and 1) for mapping purposes. Numbers closer to one represent a higher density. Dark gray areas with higher senior population density are easily identified as areas with higher needs for medical care. They are areas with higher level of risk.

The Cities of Richmond and Delta have higher senior population densities. Upcoming development decisions should be based on the spatial distribution of senior healthcare facilities for these municipalities. Providing sufficient and accessible healthcare facilities for this subpopulation are already important but as the whole region experience further increase in senior population, the level of risk that current care delivery models already experience, will increase.

3.3 Children population

Children under age 4 are recognized as a population group of increased vulnerability. Therefore, they need to be considered in the assessment of human health impacts of climate change. Figure 9 represents the population density distribution of children (4 years old and younger) for the City of Metro Vancouver. It is based on dissemination areas. The population has been normalized (between 0 and 1) for mapping. Numbers that are closer to

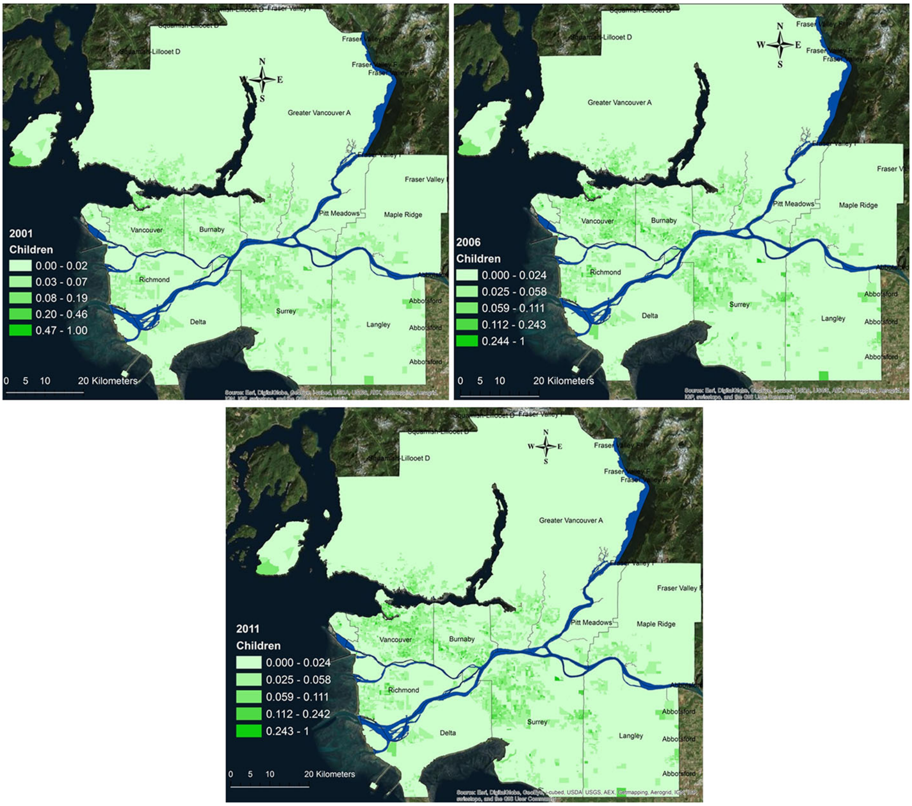

Fig. 9 Calculated normalized children population density for the City of Metro Vancouver for 2001, 2006 and 2011

one capture the areas with the higher density of this age group and hence areas of increased risk to human health in terms of hydrometeorological extremes. The cities of North Vancouver, Vancouver, Richmond and Delta have higher child populations per dissemination area.

3.4 Burden of disease

Canada is a high-income country, and infectious disease risk is generally considered low in high-income countries, this holds true for Canada. The highest infectious health risk is related to waterborne diseases as a result of drinking water contamination. Experience has shown, in higher income countries that in larger urban areas where water treatment and waste water infrastructures are well maintained and managed, the risk of waterborne infections remains low. Smaller communities with less well-developed infrastructure are at higher risk during extreme weather events as demonstrated by the Walkerton, Ontario experience (Schwartz and McConnell 2009).

DALY estimates per 100,000 population are available by country from published WHO tables (WHO 2008). While these tables address specific diseases, they are divided into three major categories, which for the purpose of mapping exercises are sufficient. These categories are communicable diseases (601 DALYs per 100,000 population), non-communicable diseases (8,799 DALYs per 100,000 population) and injuries (920 DALYs per 100,000 population). Although published as country averages, they are population based. All three categories are considered and represented based on dissemination areas. Figure 10 shows these 3 categories in 3 separate set of maps normalized between 0 and 1 for 2001, 2006 and 2011.

The map in Fig. 10 communicable diseases, is based on national averages. Figure 11 shows that non-communicable diseases constitute a higher and more widespread burden than communicable diseases, which is expected. Many of these non-communicable diseases require ongoing support from health facilities e.g., dialysis, cancer care, etc. and during extreme weather-related events, sufficiently accessible healthcare facilities need to be available to cope with this aspect of human health. Once the dynamic resilience model is in place, it will be possible to experiment with specific number of cases (for example, what will 5,000 cases of post-traumatic stress disorder (PTSD) in the non-communicable category and 50,000 cases of gastrointestinal infections (GI) illness in the communicable category post flooding do to the resilience of the city) (Figs. 11, 12).

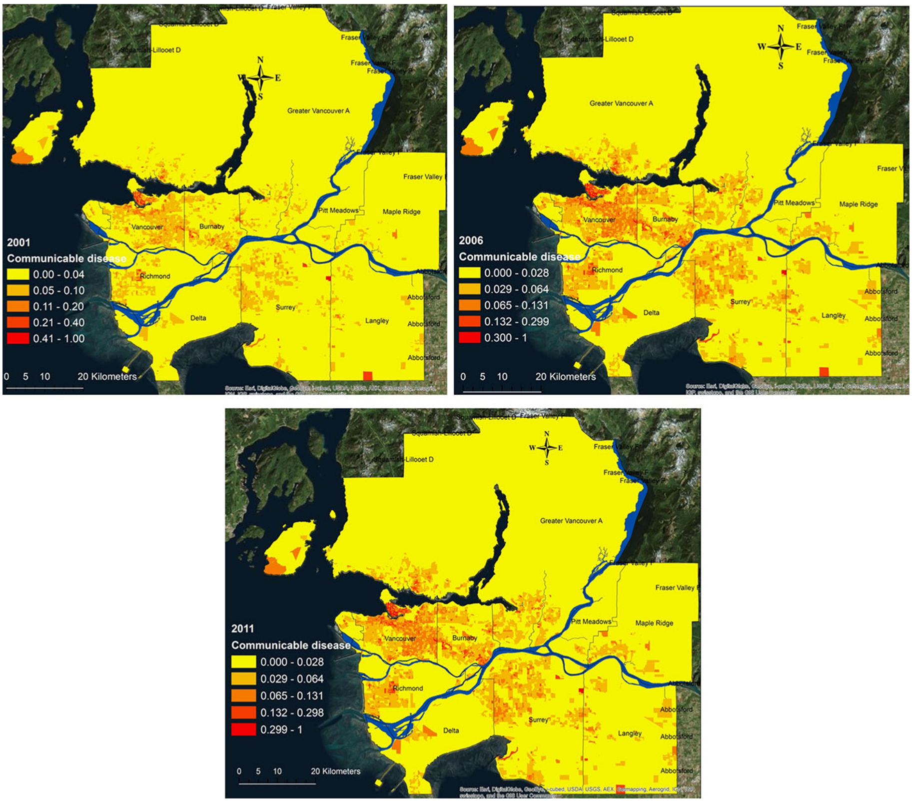

Fig. 10 Calculated normalized densities of communicable diseases for the City of Metro Vancouver for 2001, 2006 and 2011

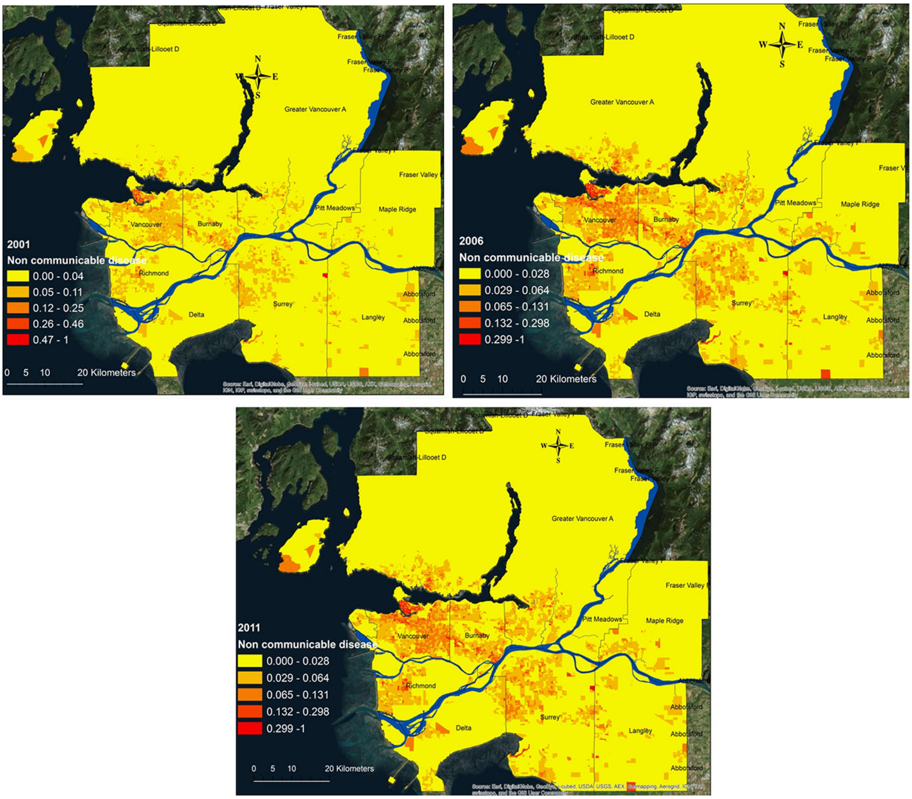

Fig. 11 Calculated normalized densities of non-communicable diseases for the City of Metro Vancouver for 2001, 2006 and 2011

3.5 Non-physical health impact map

Normalized health conditions and social conditions represented in separate maps have been integrated into one single map. The resulting map helps in identifying non-physical vulnerable regions in the City of Metro Vancouver. Figure 13 shows the map that integrates total population, population age over 65, population of children age 4 and under, communicable diseases, non-communicable diseases and injuries. This map is also normalized and rasterized. The cities of Vancouver, Richmond, Delta, Burnaby and Surrey are shown to be the regions most vulnerable in terms of non-physical health impact.

3.6 Topography

The number of flood disasters happening worldwide has grown significantly over the last few decades (Todini 1999; Kundzewicz and Schellnhuber 2004). Floods and sea level rise costs and damages are highly correlated with the topography of the area that has been exposed. It is clear the low level zones like shorelines are at high risk due to sea level rise and river flooding. This work is using topographic information as a proxy for damage due to inundation. The topographic map has been developed for the Metro Vancouver, based

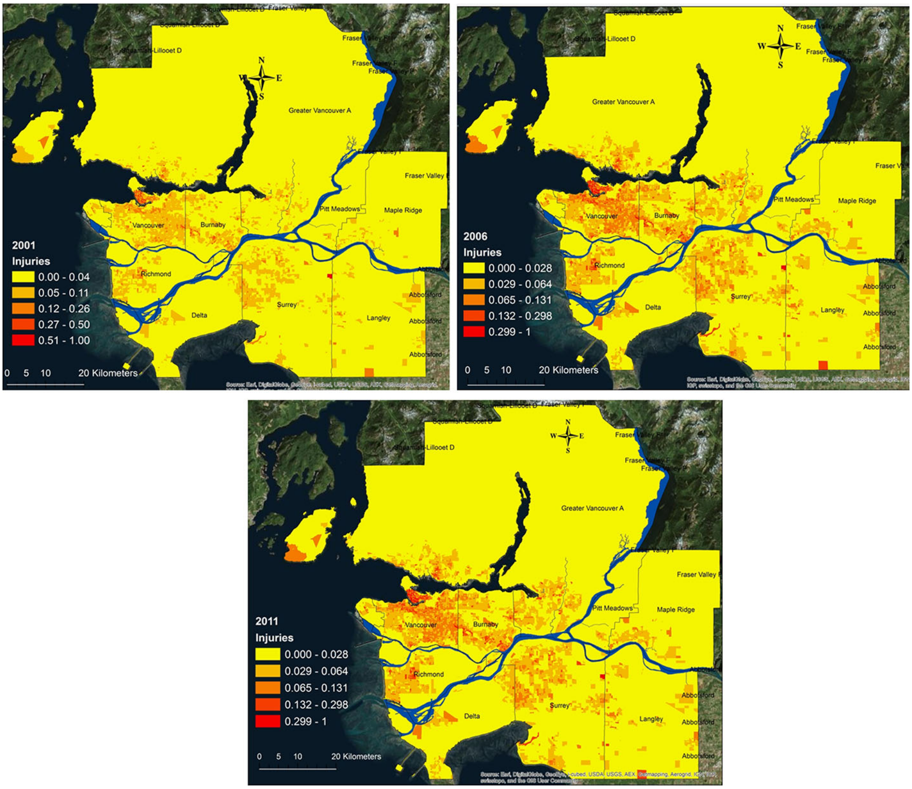

Fig. 12 Calculated normalized densities of injuries for the City of Metro Vancouver for 2001, 2006 and 2011

on the high potential risk of inundation in lower elevation regions. The map has been normalized between 0 and 1 (Fig. 14). Regions in brighter color (value closer to one) have lower elevation and are more exposed to river and sea level rise flooding. It is clear that cities like Vancouver, the south part of North Vancouver, Delta, Richmond, Coquitlam and Pitt Meadows have a high risk of inundation.

3.7 Human health impact map

The final step in the presented methodology combines the elevation map with the non-physical health impact map using Eq. 15. Figure 15 shows the final health impact map, which is also normalized between 0 and 1 for all 3 years. These three maps have been normalized together to allow for the comparison of human health impact over time. The resulting maps demonstrate clearly that Vancouver, Richmond, Delta and Surrey are more vulnerable compared to other municipalities in terms of flooding events and the impact on human health as a result.

The quantitative resilience measure combines economic, social, health and physical impacts of climate change-caused natural disasters on coastal megacities (Simonovic and Peck 2013). The paper presents an original framework for quantification of health impact which serves as one of the inputs into Coastal Megacity Resilience Simulator CMRS.

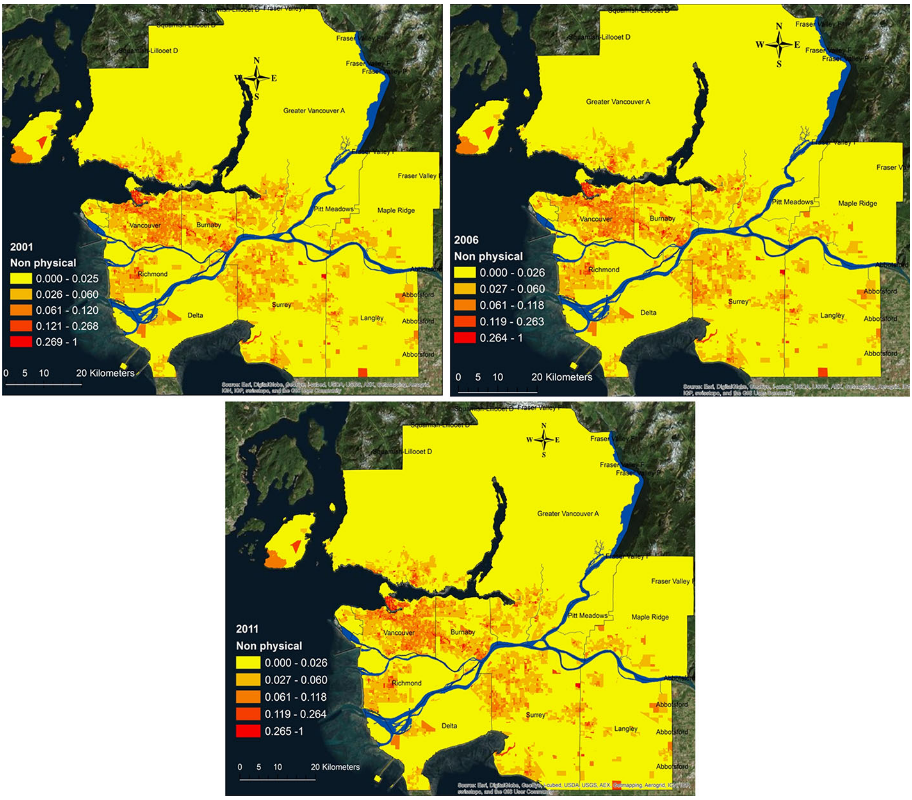

Fig. 13 Non-physical health impact map generated for the City of Metro Vancouver for 2001, 2006 and 2011

STDRM is based on time and space (Eq. 3), and human health impact maps are essential input to CMRS for assessment of city resilience.

4 Discussion

The paper shows the technique for the development of human health impact map for use with the city resilience system dynamics simulation model. The main thrust of the presented methodology is in the use of DALY estimates as a measure of the baseline burden of disease. As it is mentioned before in this research, risk is defined as the exposure of the various segments of the population to three different health impacts (communicable and non-communicable diseases, and injuries) of inundation caused by climate change-caused riverine flooding and sea level rise. The major shortcoming of this definition is apparent. The DALY estimates are for the country as a whole and not specific for urban population. However, most of the population now resides generally in urban settings. If the local knowledge of diseases that take place in higher numbers than the national average in the urban setting is available, it could be used to modify the input into the mapping process.

The data are based on population numbers, and the accuracy of this parameter varies from city to city depending on the country, for example, Vancouver has more accurate

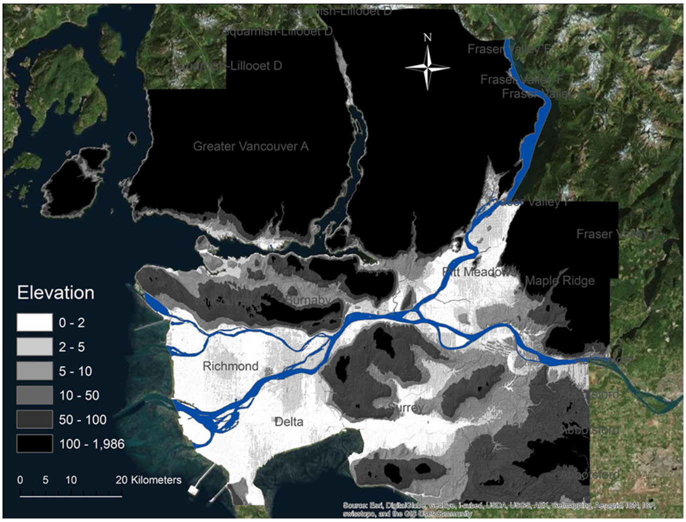

Fig. 14 Elevation map of the City of Metro Vancouver

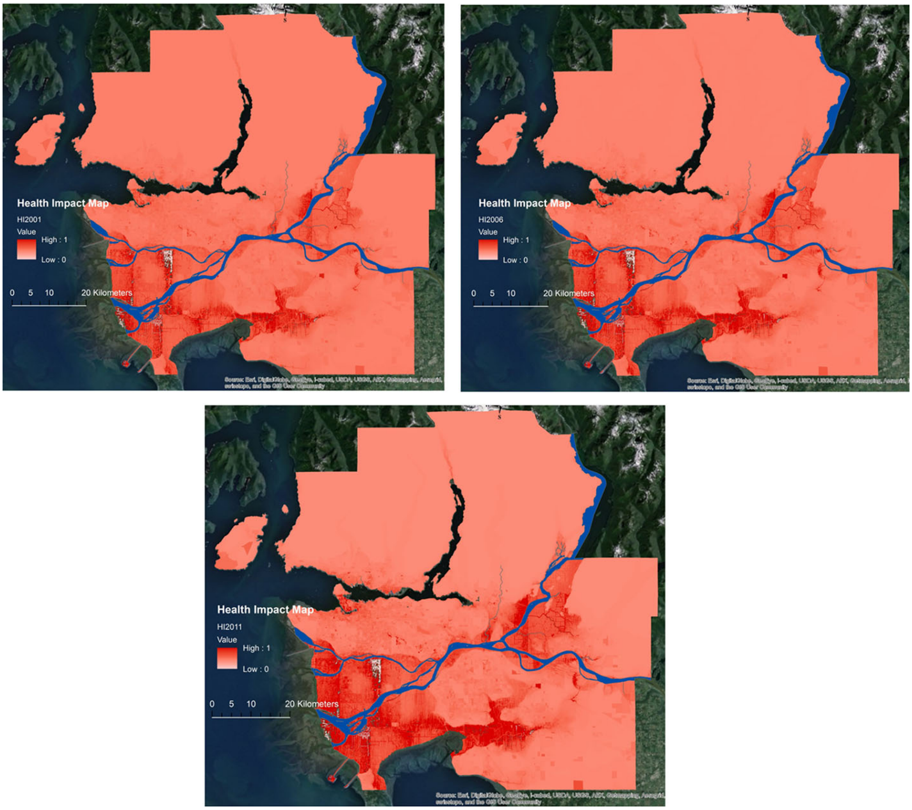

Fig. 15 Human health impact map generated for the City of Metro Vancouver for 2001, 2006 and 2011

population data than Lagos, but the goal is to use the same method for calculation of the burden of disease in all the CCaR project cities to allow for assessment of resilience in the future. The main advantage of this approach is its feasibility, and that the data are available for all the CCaR project cities. The results provide an informative picture of the baseline burden of disease in three major disease categories.

5 Conclusion

This research presents the methodology, using spatial and temporal analysis, for generating a health impact map. This tool has significant potential for selection of appropriate adaptation strategies for addressing climate change-caused natural disasters in coastal megacities. Application of the physical, health and social vulnerability assessment to climate change caused flooding using GIS, and mapping techniques have enabled a quantitative assessment of the risks of each sector and each district for the City of Metro Vancouver, Canada.

The human health impact map can be used in a stand-alone fashion to determine which regions might experience the greatest impact during the disaster. The methodology has enabled quantitative assessment of vulnerable areas using available spatial data for 3 years of 2001, 2006 and 2011. It is determined that the integrated health impact mapping approach is a necessary tool for long-term sustainable development of the coastal cities. The purpose of this tool is to assist coastal cities in developing their own risk maps and help in developing more targeted adaptation and risk reduction strategies at a local level. The methodology is flexible and allows cities to select the relevant data and change the weighting of each data input based on local concerns.

Acknowledgments The authors would like to acknowledge the financial support made available by the International Development Research Centre (IDRC) together with the Canadian Institutes of Health Research (CIHR), the Natural Sciences and Engineering Research Council of Canada (NSERC) and the Social Sciences and Humanities Research Council of Canada (SSHRC).

References

Canadian Digital Elevation Data (CDED) (2013) http://www.geobase.ca/geobase/en/about/index.html. Accessed Sept 2013

Chalabi Z, Kovats S (2014) Tools for developing adaptation policy to protect human health. Mitig Adapt Strateg Glob Change 19(3):309–330

Coastal Cities at Risk (CCaR) (2011) http://coastalcitiesatrisk.org/wordpress. Accessed May 2014

Dilley M (2005) Natural disaster hotspots: a global risk analysis, vol 5. World Bank Publications, Washington, DC

EM-DAT The International Disaster Database (2014) Center for research on the epidemiology of disasters-CRED. http://www.emdat.be/database. Accessed June 2014

EnvironmentalCanada (EC) (2007) Climate change and extreme rainfall-related flooding and surface runoff risks in Ontario. In: Cheng CS, Li G, Li Q, Auld H, Maclver D (eds) Plain language summary report. Environment Canada, Toronto

ESRI (Environmental Systems Research Inc) (2014) World Imagery, i-cubed, USDA FSA, USGS, AEX, GeoEye, Getmapping, Aerogrid, IGP

Few R and Ahern M (2004) Floods, health and climate change: a strategic review. Tyndall Centre Working Paper No. 63

Forseth P (2012) Adaptation to sea level rise in Metro Vancouver: a review of literature for historical sea level flooding and projected sea level rise in Metro Vancouver. Adaptation to Climate Change Team (ACT)

Hajat S, Ebi KL, Kovats S, Menne B, Haines A (2003) The human health consequences of flooding in Europe and the implications for public health: a review of the evidence. Appl Environ Sci Public Health 1(1):13–21

IPCC (2013) Climate Change 2013: the physical science basis. In: Stocker TF, Qin D, Plattner G-K, Tignor M, Allen SK, Boschung J, Nauels A, Xia Y, Bex V, Midgley PM (eds) Contribution of Working Group I to the fifth assessment report of the intergovernmental panel on Climate Change. Cambridge University Press, New York

Kundzewicz ZW, Schellnhuber HJ (2004) Floods in the IPCC TAR perspective. Nat Hazards 31(1):111–128

Lim SS, Vos T, Flaxman AD, Danaei G, Shibuya K, Adair-Rohani H (2010) A comparative risk assessment of burden of disease and injury attributable to 67 risk factors and risk factor clusters in 21 regions, 1990–2010: a systematic analysis for the Global Burden of Disease Study 2010. Lancet 380(9859):2224–2260

Malczewski J, Pazner M, Zaliwska M (1997) GIS-based techniques for visualizing multi criteria location analysis: a case study. Cartogr Geogr Inform Syst 24:80–90

Massam BH (1988) Multi-criteria decision making (MCDM) techniques in planning. Prog Plan 30(1):1–84

McMichael AJ (2010) Climate change, global environmental change, and health. Context, concepts and research tasks for epidemiologists. European Educational programme in Epidemiology

McMichael AJ, Woodruff R, Hales S (2006) Climate change and human health: present and future risks. Lancet 367:859–869

Milly PC, Wetherald RT, Dunne KA, Delworth TL (2002) Increasing risk of great floods in a changing climate. Nature 415:514–517

Nirupama N, Armenakis C, and Montpetit M (2014) Is flooding in Toronto a concern? Nat Hazards 72(2):1259–1264

Population data (2014) www.popdata.bc.ca. Accessed July 2013

Prüss-Üstün A, Mathers C, Corvalán C and Woodward A (2003) Introduction and methods: assessing the environmental burden of disease at national and local levels. Geneva, World Health Organization, (WHO Environmental Burden of Disease Series, No. 1)

Schmidt W, Skala M, Donelon I, Donnell HD (1993) Morbidity surveillance following the Midwest flood—Missouri. MMWR 42:797–798

Schwartz R, McConnell A (2009) Do crises help remedy regulatory failure? A comparative study of the Walkerton water and Jerusalem banquet hall disasters. Can Public Adm 52(1):91–112

Simonovic SP (2011) Systems approach to management of disasters: methods and applications. Wiley, Hoboken

Simonovic SP, Peck A (2013) Dynamic resilience to climate change caused natural disasters in coastal megacities quantification framework. Br J Environ Clim Change 3(3):378–401

Statistics Canada (2012) Greater Vancouver, British Columbia (Code 5915) and British Columbia (Code 59). Census Profile. Statistics Canada Catalogue no. 98-316-XWE. Ottawa

The Organization for Economic Co-operation and Development (OECD) (2013) http://www.oecd.org/newsroom/future-flood-losses-in-major-coastal-cities.html. Accessed May 2014

Todini E (1999) An operational decision support system for flood risk mapping, fore casting, and management. Urban Water 1(2):131–143

Turcotte M and Schellenberg M (2006) A Portrait of Seniors in Canada. Published by authority of the Minister responsible for Statistics Canada, Catalogue no. 89-519-XIE ISBN 978-0-662-45047-4

Waroux OP (2011) Foolds and human health risks. Center for research on the Epidemiology of Disasters, Brussels

World Health Organization (WHO) (2008) The global burden of disease: 2004 update. Geneva, WHO, www.who.int/evidence/bod. Accessed May 2013

World Health Organization (WHO) (2010) Piloting climate change adaptation to protect human health. World Health Organization, Geneva, http://www.who.int/globalchange/climate/gefproject/en/index.html. Accessed April 2014

Young T, Tucker T, Galloway M, Manyike P, Chapman A, and Myers J (2010) Climate change and health in SADC region: review of the current state of knowledge. Centre for Occupational and environmental Health Research